Research on Identification of LVRT Characteristics of Photovoltaic Inverters Based on Data Testing and PSO Algorithm

Authors:

Pingping Han, Guijun Fan, Weizhen Sun, Bolong Shi, Xiaoan Zhang

Date Submitted: 2019-07-29

Keywords: LVRT, PV inverter, particle swarm optimization algorithm, real operation data, parameter identification

Abstract:

With the continuous increment of photovoltaic (PV) energy connection into a power grid, the accuracy of control parameters of PV power generation systems becomes the key to the stable operation of the power grid. At present, parameter identification based on an intelligent algorithm is a common means to obtain control parameters. However, most of the data used for identification are simulation data and the identified parameters are difficult to use in practical engineering. Therefore, aiming at the acquisition of low voltage ride through (LVRT) control parameters of PV unit, a method of identification of LVRT parameters of the PV unit is proposed, which combines sensitivity analysis with field measurement. In this paper, the test scheme of the required data is put forward through sensitivity analysis of the identified parameters, and the intelligent algorithm is used to identify the low voltage traverse parameters of the data. Finally, the optimal value is extracted from the identification results and substituted into the model. The accuracy of the parameter identification results is verified by calculating the error between the output of the model and the real operation data. The method considers the errors caused by different power levels of the inverters with highly accurate and consistent identification results, which is applicable to practical engineering calculation.

Record Type: Published Article

Submitted To: LAPSE (Living Archive for Process Systems Engineering)

Citation (overall record, always the latest version):	LAPSE:2019.0815
Citation (this specific file, latest version):	LAPSE:2019.0815-1
Citation (this specific file, this version):	LAPSE:2019.0815-1v1

DOI of Published Version: https://doi.org/10.3390/pr7050250

processes

MDPI

Article

Research on Identification of LVRT Characteristics of Photovoltaic Inverters Based on Data Testing and PSO Algorithm

Pingping Han [1], Guijun Fan [1,*], Weizhen Sun [2], Bolong Shi [2] and Xiaoan Zhang [3]

[1] Anhui Provincial Laboratory of New Energy Utilization and Energy Conservation, Hefei University of Technology, Hefei 230009, China; LH021211@163.com
[2] State Grid Zhejiang Electric Power Company, Hangzhou 310000, China; sun_weizhen@zj.sgcc.com.cn (W.S.); shi_bolong@zj.sgcc.com.cn (B.S.)
[3] Institute of Intelligent Manufacturing, Hefei University of Technology, Hefei 230009, China; zhangxiaoan@263.net
* Correspondence: Fan_fan1995@163.com; Tel.: +86-1822-560-5806

Received: 19 March 2019; Accepted: 26 April 2019; Published: 29 April 2019

Abstract: With the continuous increment of photovoltaic (PV) energy connection into a power grid, the accuracy of control parameters of PV power generation systems becomes the key to the stable operation of the power grid. At present, parameter identification based on an intelligent algorithm is a common means to obtain control parameters. However, most of the data used for identification are simulation data and the identified parameters are difficult to use in practical engineering. Therefore, aiming at the acquisition of low voltage ride through (LVRT) control parameters of PV unit, a method of identification of LVRT parameters of the PV unit is proposed, which combines sensitivity analysis with field measurement. In this paper, the test scheme of the required data is put forward through sensitivity analysis of the identified parameters, and the intelligent algorithm is used to identify the low voltage traverse parameters of the data. Finally, the optimal value is extracted from the identification results and substituted into the model. The accuracy of the parameter identification results is verified by calculating the error between the output of the model and the real operation data. The method considers the errors caused by different power levels of the inverters with highly accurate and consistent identification results, which is applicable to practical engineering calculation.

Keywords: parameter identification; real operation data; particle swarm optimization algorithm; LVRT; PV inverter

1. Introduction

Accurate modeling of photovoltaic (PV) power generation systems is the basis of analyzing the stability of a power grid. An inverter is the core component of a PV power generation system, and the accuracy of its model depends on the accuracy of the control parameters obtained. As a part of the control parameters of the inverters, the low voltage ride through (LVRT) control parameters are important to ensure the continuous operation of the PV system under voltage drop conditions. During the period of power grid failure, if the deviation of LVRT control parameters is large, the inverters cannot provide the correct reactive power, which may lead to the failure of the inverters, making the grid-side overcurrent, direct-current (DC) side overvoltage, or even causing large-scale disconnection and serious transfer of power flow in the system, resulting in the loss of guiding significance of simulation results for real operation. Therefore, the accurate acquisition of LVRT control parameters is very important. However, in general, because of factories' confidentiality or changes in operating

environments, it is impossible to ensure the accuracy of control parameters, thus affecting the accurate analysis of grid-connected characteristics of single inverters and PV stations.

At present, the main way to accurately obtain the simulation parameters of a new energy system is to identify the parameters of the model with the real operation data and appropriate algorithms. The commonly used methods to obtain parameters are theoretical analysis and system identification. The theoretical analytic method can reproduce the internal process of the PV system to the greatest extent. However, as the control system becomes more and more complex, the nonlinear calculus equation brings great difficulties to the calculation, and some unmeasurable variables will affect the calculation results. As a result, the obtained parameters often need to be adjusted many times before they can be used in PV control [1]. The system identification method uses the input and output of the model to solve unknown parameters, including the time domain identification method [2], the frequency domain identification method [3], and the intelligent optimization method [4–7]. The time domain identification method first sampled and analyzed the time domain information of the system, and then identified the unknown parameters according to the time domain sampling information. The commonly used method is the least square method [8]. The frequency domain identification method first converts the time domain information of the system to the frequency domain according to the fast Fourier change, and then identifies the unknown parameters according to the frequency response characteristics of the system [9]. Intelligent optimization algorithm is widely used. It is based on the global optimization characteristics of the algorithm itself, calculating the fitness of the objective function to determine the optimal value of model parameters. The commonly used intelligent optimization algorithms are the ant colony algorithm [10], particle swarm optimization [11], and genetic algorithm [12].

Intelligent optimization algorithm has been widely used in the field of power system parameter identification, such as in the works of [13–16]. In identification data, most of the existing studies use simulation data to verify the validity of the identification algorithm, but simulation data cannot be applied to parameter identification of actual engineering. In identification methods, the existing research focuses on the validation of single parameter identification methods, and does not consider how to extract the optimal results from multiple identification results, which is of low practical value. Moreover, the existing reference only identifies the parameters of PV array, the parameters of PI control link, and the limiting link of PV inverters [17–21]. There is no report on the identification of LVRT control parameters of the PV power generation system. In view of the above situation, this paper obtains the real test data by designing the test scheme, and identifies the LVRT control parameters of PV inverters multiple times using the real test data, which makes up for the shortcoming that most of the existing literature uses simulation data to identify, but cannot solve the practical engineering problems. Multiple identification can adapt to the randomness of the operating environment, and is more reliable than the single identification result.

In this paper, a parameter identification method for LVRT control of PV units is proposed, which combines sensitivity analysis with real test scheme. Firstly, the sensitivities of the parameters to be identified in PV units are analyzed, and the test scheme of the data to be identified is proposed. Then, the adaptive inertia weight particle swarm optimization algorithm and multi-group real operation data are used to identify the LVRT control parameters of the grid-connected PV system, and the optimal values are extracted from the multi-group identification results. Finally, the optimal values are substituted into the model and the error between the output of the model and the actual measurement is calculated to verify the accuracy of parameter identification results.

2. Introduction of Parameters to be Identified

2.1. Low Voltage Ride Through Requirements

LVRT control is an important part of the control system of grid-connected PV inverters. In order to ensure the stable operation of the grid-connected PV system during the voltage sag of the grid,

the state promulgated the relevant national standard GB/T 19964-2012 "Technical Regulations for the Access of Photovoltaic Stations to Power Systems", which stipulates the grid-connected curve during the LVRT period, as shown in Figure 1.

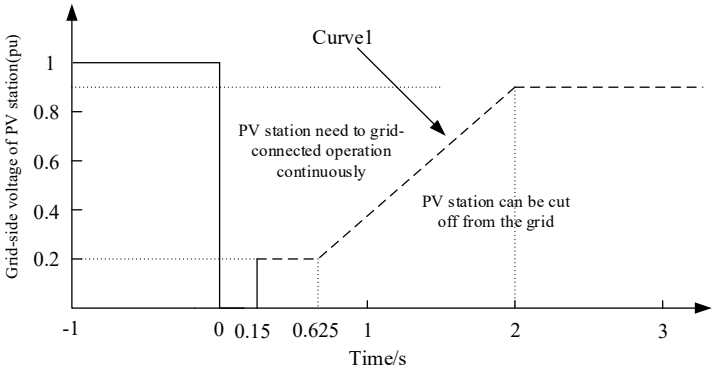

Figure 1. The requirement of low voltage ride through (LVRT) for photovoltaic (PV) power plants.

As can be seen from the above analysis, when the grid-connected point voltage drops as a result of the power system fault and the grid-connected voltage of PV power generation system is above curve 1, the system needs to maintain uninterrupted grid-connected operation; when the grid-connected point voltage drops to zero, the system should keep the grid-connected state running for 0.15 s continuously; when the grid-connected voltage drops below the curve, beyond the fault crossing requirements, the PV power generation system should cut out of the grid and stop sending electricity.

2.2. Control Strategy and Structure of Low Voltage Ride Through

When a voltage drop fault occurs on the grid-side, the PV inverters switch the control mode according to the degree of voltage sag: normal control strategy–LVRT control strategy–normal control strategy, as shown in Figure 2.

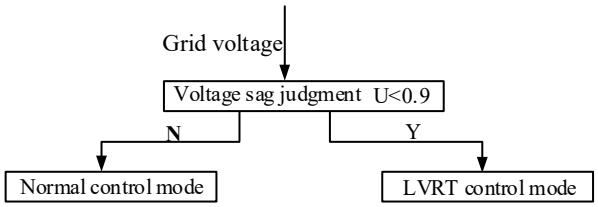

Figure 2. Control switching flow chart of inverter.

In order to ensure the realization of LVRT, during the voltage drop period, the inverters need to realize the priority control of reactive power according to the grid-side voltage, and send out reactive power to support the grid voltage recovery. The specific LVRT control structure is shown in Figure 3.

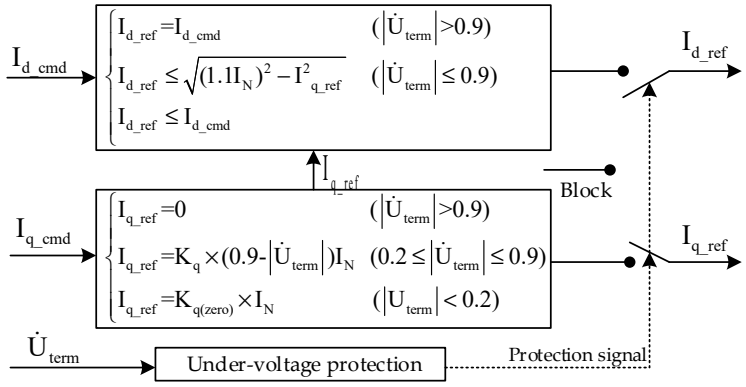

Figure 3. LVRT control.

I_{q_ref} is the reference value of reactive current, I_{d_ref} is the reference value of active current, $Id_{\_cmd}$ is the output active current of inverters, I_{q_cmd} is the output reactive current of inverters, I_N is the rated current, U_{term} is the per-unit value after voltage sag at grid-connected points, and K_q is the reactive current support coefficient during LVRT. $K_{q\,(zero)}$ is the support coefficient of reactive current when zero voltage passes through.

For PV power generation systems that are not off-grid during the fault period, the active power should be restored to normal working state at a rate of at least 30% rated power per second after the fault is cleared, this value is reflected in the simulation model by the parameters of the active current recovery slope of PV.

2.3. Low Voltage Ride Through Parameters to be Identified for Photovoltaic Unit

For PV inverters, the active current recovery slope determines the speed of active power recovery after fault clearance and the reactive current support coefficient determines the amount of reactive power generated by the inverters during the fault period, which are key control parameters during the LVRT period. Although the control structures of different brands of inverters in the market are similar, the specific control parameters are different, which leads to great differences in LVRT characteristics. Therefore, it is necessary to identify the active current recovery slope and reactive current support coefficient to obtain the LVRT control parameters required by the simulation model, as shown in Table 1.

Table 1. Contents to be tested. LVRT—low voltage ride through; PV—photovoltaic.

Test Object	Parameters to be Identified	Parameters' Meanings
PV Inverter	LVRT control parameters: Kq, dIp	Kq: reactive current support coefficient dIp: active current recovery slope

3. Design for Data Testing Scheme

Through sensitivity analysis, the degree of correlation between system parameters and external characteristics can be understood, and the test scheme can be designed according to the degree of correlation to obtain the real operation data needed for parameter identification.

3.1. Trajectory Sensitivity Analysis of Parameters to be Identified

3.1.1. Trajectory Sensitivity

The trajectory sensitivity refers to the degree to which the external characteristics of the system are sensitive to changes in system parameters or surrounding conditions. The expression of trajectory sensitivity is as follows:

$$S_{\theta_i} = \lim_{\Delta\theta_i \to 0} \frac{\frac{y(t,\theta_1,\ldots,\theta_i+\Delta\theta_i,\ldots,\theta_m)-y(t,\theta_1,\ldots,\theta_i,\ldots,\theta_m)}{y(t,\theta_1,\ldots,\theta_i,\ldots,\theta_m)}}{\frac{\Delta\theta_i}{\theta_{i0}}}, \quad (1)$$

where $S_{\theta i}$ is the trajectory sensitivity of the i-th parameter θ_i, θ_{i0} is the given value of the parameter θ_i, y is one of the observed quantities, and m is the number of parameters to be identified.

Generally, the sensitivity calculation can be used to estimate the degree of correlation between system parameters and external characteristics, which is helpful to determine the identifiability of parameters. "The greater the disturbance, the higher the accuracy of parameter identification" [22], that is, the parameters with high sensitivity are easy to identify and the identification accuracy is high, whereas the parameters with small sensitivity are difficult to identify and the identification accuracy is low.

3.1.2. Sensitivity Analysis

In this paper, the active power and reactive power at the grid-connected point of the PV power generation system are selected as observed quantity, the sensitivity of active current recovery slope, and reactive current support coefficient are calculated, and the correlation degree of the observed quantity to the identification parameters is analyzed. The PV model used can be found in Guidelines for Modeling of PV Power Systems GB/T 32826-2016.

Set the power reference value as shown in Figure 4, and the sensitivity of the parameters to be identified is shown in Figure 5.

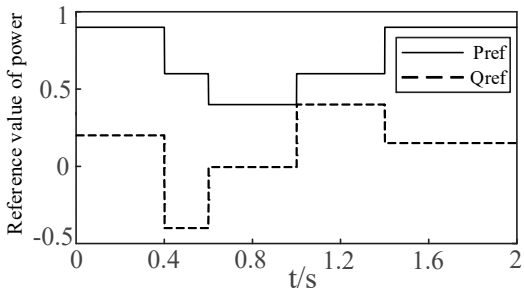

Figure 4. Reference value of power of the converter.

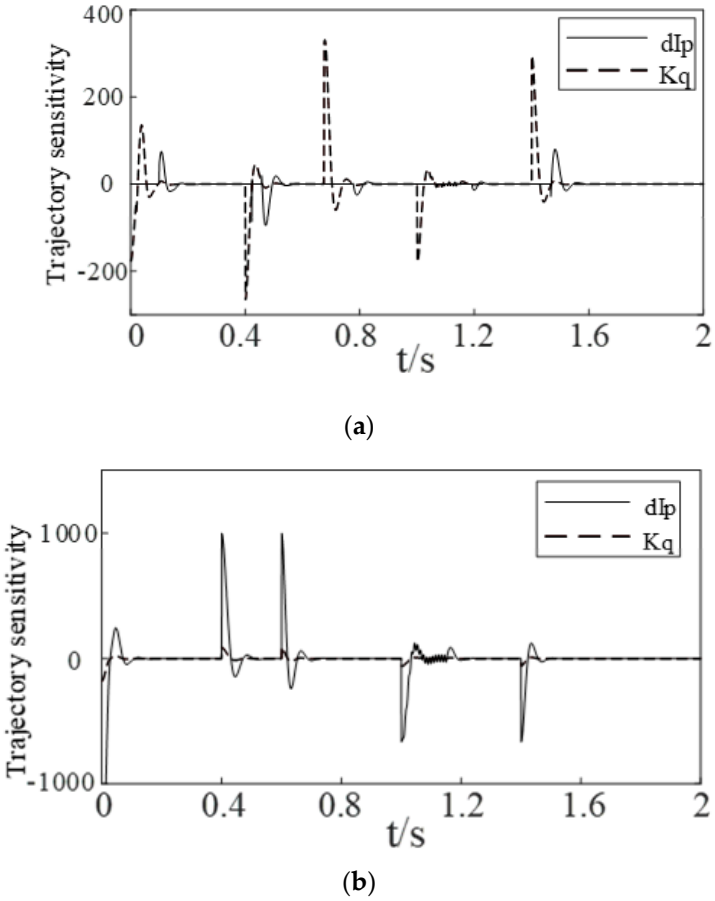

Figure 5. Sensitivity curve of the parameter to be identified: (**a**) sensitivity curve of active power of the parameter to be identified; (**b**) sensitivity curve of reactive power of the parameter to be identified.

From the trajectory sensitivity shown in Figure 5, it can be seen that the response of active current recovery slope is intense and the response of reactive current support coefficient is small at the instant of active power change, while the response of reactive current support coefficient is intense and the response of active current recovery slope is small at the instant of reactive power change. It can be concluded that active power is highly sensitive to active current recovery slope and reactive power is highly sensitive to reactive current support factor. On this basis, a test scheme can be designed, as shown in the next section.

3.2. Test Scheme

The test platform is a 1000 kW PV power generation system, and the test point is the alternating current (AC) side of the inverter, as shown in Figure 6. The model of the inverters to identify the LVRT control parameters is CP-1000-B, and the internal parameters are shown in Table 2.

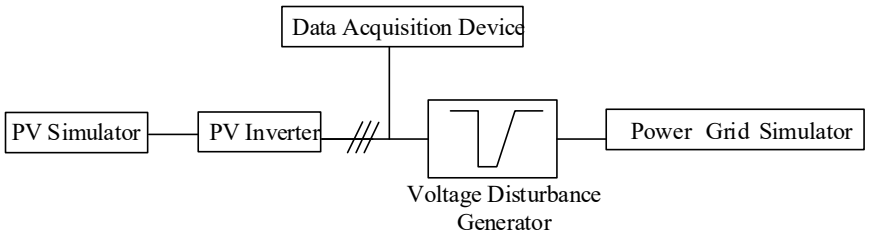

Figure 6. Diagram of test platform.

Table 2. Parameters of photovoltaic inverters to be measured.

DC Side Parameters	Direct current (DC) Bus Start Voltage (Vdc)	500
	Minimum DC Bus Voltage (Vdc)	300
	Maximum DC Bus Voltage (Vdc)	850
	Full load Maximum Power Point Tracking (MPPT) voltage range (Vdc)	750~820
	Optimum MPPT Operating Point Voltage (Vdc)	780
	DC Bus Capacitor (μF)	12,600
Alternating Current (AC) Side Parameters	Rated output power (kW)	1000
	Maximum output power (kW)	1100
	Rated grid-side voltage (Vac)	520
	Allowable voltage range at grid-side (Vac)	468~572 (Settable)
	Rated grid frequency (Hz)	50
	Allowable frequency range of power grid (Hz)	45~55
	AC side rated output current (A)	1110
	Power factor (leading~lagging)	leading 0.9~lagging 0.9

Direct power control is adopted in PV inverters to achieve a fast power control response. The basic control ideas are as follows: Firstly, the instantaneous active power and instantaneous reactive power of PV grid-connected inverters are detected and calculated. Secondly, the deviation between the measured value and the given instantaneous power reference value is fed into the controller. Thirdly, the switching state of the switch is determined according to the output of the controller and the judgment of the voltage vector position of the power grid.

According to the GB/T32892-2016 "Photovoltaic Power System Model and Parameter Test Rules", the grid-side disturbance experiment is carried out in three sets of active power range, and six sets of test conditions are set. The three sets of active power range are as follows: (a) high power output range: P > 0.7 Pn; (b) intermediate power output range: 0.5 Pn = < P < 0.7 Pn; (c) 0.1 Pn =<P < 0.5 Pn. Therefore, the active power instructions in the test scheme are set to 0.2 Pn, 0.6 Pn, and 0.8 Pn respectively, and the voltage disturbances are set by voltage disturbance generator devices, which are 0.1 Un, 0.4 Un, 0.7 Un, and 0.8 Un, respectively, as shown in Table 3.

Table 3. Test cases.

Operating Mode	P/pu	U/pu	Test Data
1	0.2	0.1	P,Q,U
2	0.2	0.4	P,Q,U
3	0.6	0.4	P,Q,U
4	0.6	0.7	P,Q,U
5	0.8	0.7	P,Q,U
6	0.8	0.8	P,Q,U

3.3. Real Operation Data for Identification

The six working conditions in Table 3 are tested one by one on the test platform. The instantaneous active power reference value of PV inverters and the disturbance parameters of voltage disturbance generator on AC-side of PV inverters are set respectively according to the six working conditions in

Table 3. The reference value of reactive power is set to 0 uniformly. After setting up the working condition, the transient simulation of the test platform is carried out to complete all the working conditions and collect electrical data under six working conditions: the fundamental component of the grid-side voltage, the per-unit value of active power, and the per-unit value of reactive power. The characteristic curve is shown in the Figure 7.

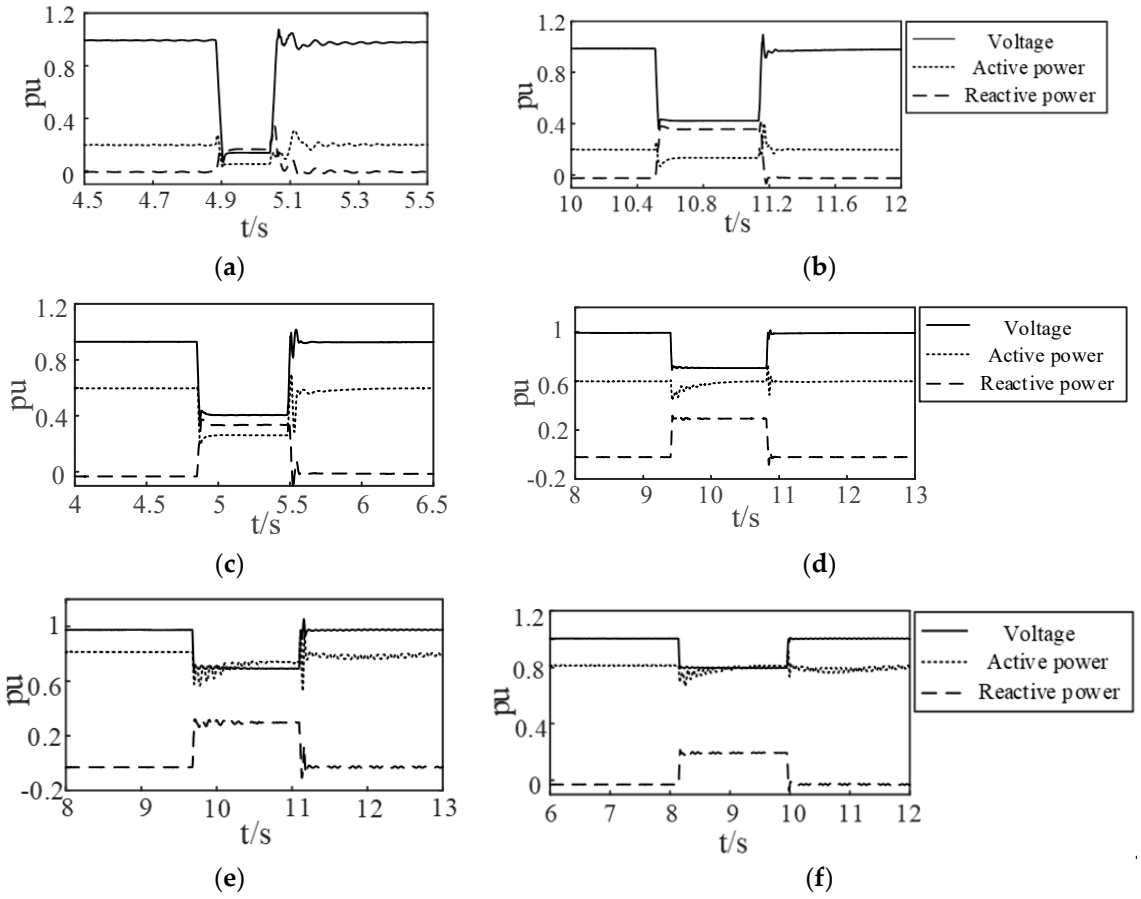

Figure 7. Diagram of electrical variables in real test data: (**a**) operation mode 1; (**b**) operation mode 2; (**c**) operation mode 3; (**d**) operation mode 4; (**e**) operation mode 5; (**f**) operation mode 6.

4. Adaptive Weighted Particle Swarm Optimization

Among the adjustable parameters of particle swarm optimization algorithm, inertia weight is the most important parameter. Because the particle swarm optimization algorithm is prone to lose population diversity and local convergence in the later stage of operation, the larger inertia weight is conducive to the global search ability of the algorithm, while the smaller inertia weight is conducive to enhance the local search ability of the algorithm. Therefore, the inertia weight based on the dynamic change of particle operation state is conducive to the improvement of the search ability of the algorithm. According to different weight change formulas, different particle swarm optimization algorithms can be obtained, such as the linear decreasing weight method, adaptive weight method, and random weight method [23].

In this paper, the adaptive weighted particle swarm optimization (AWPSO) algorithm is used to identify the parameters. The expression of inertia weight is as follows:

$$w = \begin{cases} w_{min} - \frac{w_{max} - w_{min} \times (f - f_{min})}{f_{avg} - f_{min}} & , f \le f_{avg} \\ w_{max} & , f > f_{avg} \end{cases}. \quad (2)$$

In the formula, w_{max} and w_{min} are the maximum and minimum values of w, respectively, which are generally set to 1.2 and 0.4, respectively, representing the current objective function values of particles. f_{avg} and f_{min} represent the average and minimum objective values of all particles, respectively. In the above formula, the inertia weight changes automatically with the particle's objective function value, which not only balances the global search ability and local improvement ability of particle swarm optimization, but also has high accuracy in parameter identification. The identification process of LVRT parameters based on the AWPSO algorithm is shown in Figure 8.

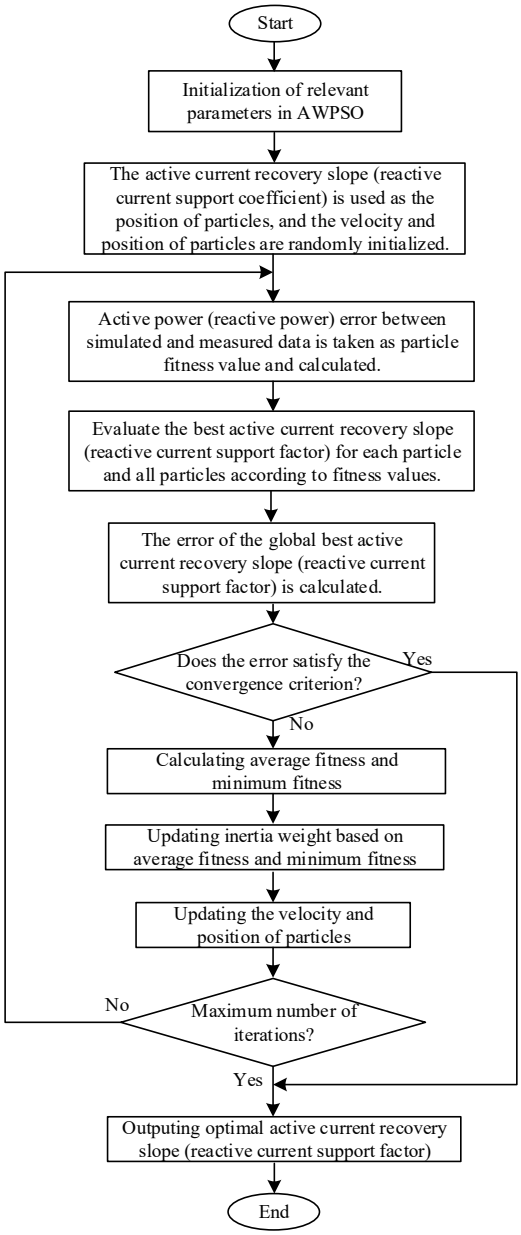

Figure 8. Flow chart of parameter identification. AWPSO—adaptive weighted particle swarm optimization.

5. Case Study

The LVRT control parameters are identified by the real test data collected under six typical working conditions on the test platform. A single-stage grid-connected PV model is built by MATLAB/simulink simulation platform (R2018a, mathworks, Natick, MA, USA, 2018), in which the parameters of the inverters are shown in Table 2.

5.1. Identification Results

The data of six typical working conditions are identified and the preliminary results of parameter identification are shown in Table 4.

Table 4. Preliminary result of parameter identification.

Operating Mode/Parameter	Active Current Recovery Slope (dIp)	Reactive Current Support Coefficient (Kq)
1	19.56254	1.441337
2	19.97261	1.769143
3	1.97195	1.672297
4	20.05121	2.13746
5	0.455699	2.077852
6	20	2.377938

In Table 4, the real operation data under each working condition correspond to a set of parameters to be identified.

5.2. Calculation and Analysis of Errors

In order to extract the most suitable parameters for all working conditions from the six sets of parameters in Table 2, the parameters corresponding to each working condition are substituted into the model respectively, and the errors between the output of the model and the corresponding test operation data are calculated.

5.2.1. Error Formula

According to GB/T 32892-2016 "Photovoltaic Power System Model and Parameter Testing Rules", the disturbance process can be divided into three intervals, namely, the pre-disturbance, the time-disturbance, and the post-disturbance, as shown in Figure 9.

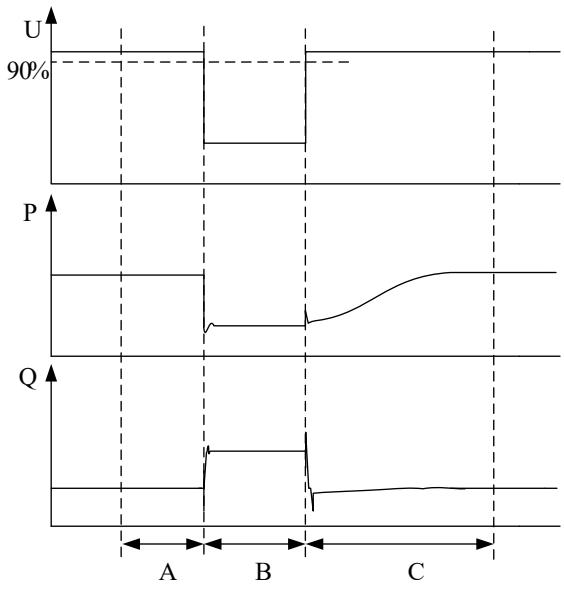

Figure 9. Diagram of division of disturbance intervals.

The formula for calculating the deviation of each interval is as follows:

$$F_n = \left| \frac{1}{K_{S\_End} - K_{S\_START} + 1} \sum_{i=K_{S\_START}}^{K_{S\_End}} X_S(i) - \frac{1}{K_{M\_End} - K_{M\_START} + 1} \sum_{i=K_{M\_START}}^{K_{M\_End}} X_M(i) \right|. \quad (3)$$

In the formula, F_n represents the deviation of each interval; and n = 1, 2, 3 represent the pre-disturbance, the time-disturbance, and the post-disturbance, respectively. X_S is the per-unit value of model simulation data for electrical quantity to be assessed. XM is the per-unit value of the test operation data of the electrical quantity to be assessed. K_{S_Start} and K_{S_End} are the first and last serial numbers of model simulation data in the calculation error interval, respectively. K_{M_Start} and K_{M_End} are the first and last serial numbers of the test operation data in the calculation error interval, respectively. The electrical quantities to be assessed are the fundamental component of grid-side voltage, active power, reactive power, reactive current, and total current.

The weighted mean deviations of the three intervals are as follows:

$$F_G = 0.1 \times F_1 + 0.6 \times F_2 + 0.3 \times F_3, \tag{4}$$

where F_G is the weighted average total deviation of all intervals.

The formula for calculating relative error is shown in Formula (5):

$$\text{error} = \frac{x_1 - x_{min}}{x_{min}}. \tag{5}$$

In the formula, x_1 is the weighted average deviation of active power and reactive power, which is an n × 2n dimension matrix; the first n column is classified as the weighted average deviation of active power, and the second n column is classified as the weighted average deviation of reactive power; x_{min} is the minimum value of weighted average deviation of active power or reactive power under the same operating conditions, which is an n × 1 order matrix; and error is the relative error of weighted mean deviation.

5.2.2. Error Formula

The optimum parameters are extracted from the preliminary identification results of six sets of parameters obtained using the real operation data under six working conditions. According to Formula (3) and Formula (4), the weighted average deviations of active power and reactive power are calculated respectively and the relative errors of the weighted average deviations of active power and reactive power corresponding to each group of parameters are calculated. According to the working condition corresponding to the minimum relative errors of the weighted average deviations of active power, the active current recovery slope corresponding to the working condition is selected as the optimal parameter and according to reactive power and according to the working condition corresponding to the minimum relative error of the weighted average deviation of reactive power, the reactive current support coefficient corresponding to the working condition is selected as the optimal parameter. Finally, the optimal parameters are determined: dIp = 20, Kq = 1.769143.

By substituting the optimal parameters obtained from the current calculation into the model and comparing simulation data with the real operation data, it can be seen that the simulation values can approximate the real operation curves by comparing the electrical quantity of the simulation values and the real operation values under the six working conditions shown in Figure 10.

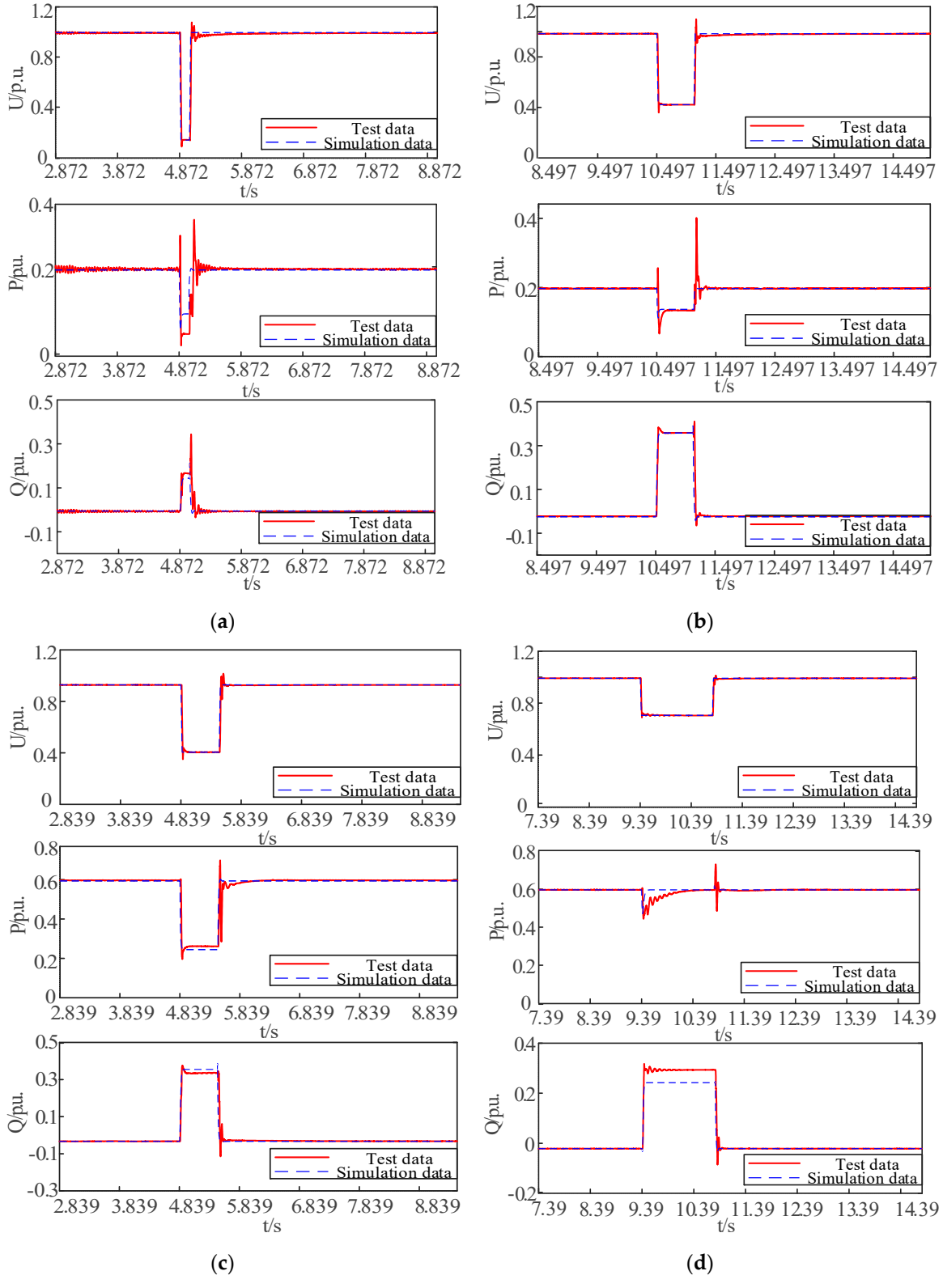

Figure 10. *Cont.*

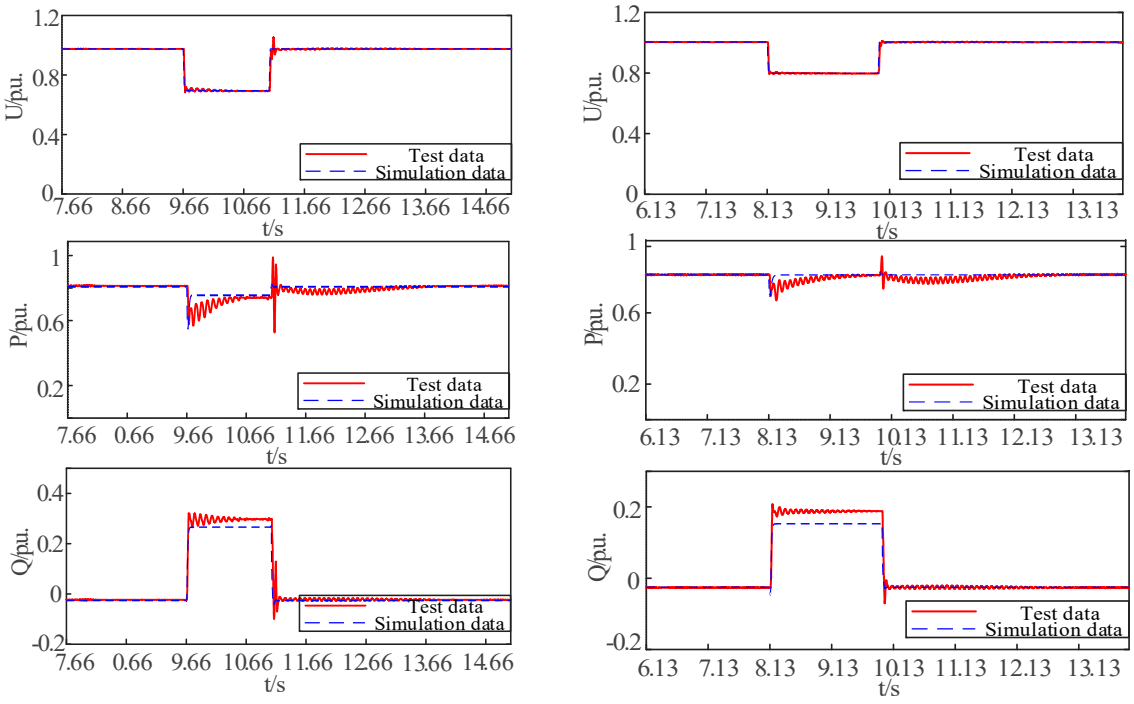

Figure 10. Contrast diagram between simulated data and real test data: (**a**) contrast diagram between simulated data and real test data under operation mode 1; (**b**) contrast diagram between simulated data and real test data under operation mode 2; (**c**) contrast diagram between simulated data and real test data under operation mode 3; (**d**) contrast diagram between simulated data and real test data under operation mode 4; (**e**) contrast diagram between simulated data and real test data under operation mode 5; (**f**) contrast diagram between simulated data and real test data under operation mode 6.

As can be seen from Figure 10, the simulation data can approximate the real test data under most operating modes. Therefore, in order to directly judge the accuracy of parameters, the weighted average deviations of five electrical quantities under six working conditions are calculated according to formulas (3) and (4). The error results are as Table 5.

Table 5. Weighted mean deviation.

Operating Mode\Deviation	Voltage Deviation	Current Deviation	Active Power Deviation	Reactive Current Deviation	Reactive Power Deviation
1	0.0468	0.0290	0.0324	0.0743	0.0140
2	0.0097	0.0437	0.0391	0.0942	0.0403
3	0.0085	0.0078	0.0374	0.0719	0.0308
4	0.0033	0.0239	0.0165	0.0809	0.0573
5	0.0050	0.0410	0.0506	0.0793	0.0558
6	0.0024	0.0220	0.0224	0.0580	0.0465

Referring to GB/T32892-2016 "Photovoltaic Power System Model and Parameter Test Rules", the upper limit of weighted average deviation of voltage in error range is 0.05 and the upper limit of weighted average deviation of total current, active power, reactive power, and reactive current is 0.15. Table 5 shows that although the error of simulation comparison chart under some working conditions is large, the specific error is within the allowable range of the national standard. It verifies the strategy is feasible by designing a test scheme to obtain the real test data instead of the simulation data to identify the parameters and extracting the optimal value of the minimum relative error from the identification results of multiple measured data. The obtained identification results are more adaptable to the randomness of the operating environment and applicable to the actual typical working conditions.

6. Conclusions

In view of the determination of LVRT parameters for PV units, this paper proposes a parameter identification method based on sensitivity analysis and test scheme, which is important for accurate modeling of a grid-connected PV system. The conclusions obtained in this paper and issues that require further study include the following:

(1) The key to accurate modeling of a PV grid-connected system is that the data used for parameter identification are consistent with the real operation data. On the basis of the results of sensitivity analysis of parameters, this paper designs a test scheme to obtain the real test data, and uses the real test data to replace the simulation data for parameter identification, which ensures the validity of parameter identification data and makes the result of parameter identification more conducive to practical engineering application.

(2) From the six sets of parameters identified from six sets of real test data in this paper, the operation conditions have a greater impact on the identification results. This paper identifies the parameters of several sets of real test data, and extracts the optimal parameters that minimize the relative errors of six sets of working conditions from the identification results. Compared with the single identification results, the multiple identification results are more suitable for the random operation environment. The identification results are more reliable.

(3) Taking the actual PV inverter model as an example, the LVRT control parameters are identified. The simulation curve of parameter identification results can approximate the measured data, which verifies the effectiveness of the method described in this paper.

(4) In this paper, a general model is used to identify the LVRT parameters. If other control needs to be studied, the test scheme and algorithm need to be further improved.

Author Contributions: This paper was a collaborative effort between the authors. The authors contributed collectively to the collation and review of literatures. P.H. and W.S. conceived and designed experiments. B.S. provided an experimental platform. X.Z. collected and collated references. G.F. performed the experiments and wrote the papers.

Funding: This research was funded by Science and Technology Foundation of State Grid Corporation of China, grant number 52110417000F.

Conflicts of Interest: The authors declare no conflict of interest.

Nomenclature

PV	photovoltaic
LVRT	low voltage ride through
PSO	particle swarm optimization
AWPSO	adaptive weighted particle swarm optimization
Kq	reactive current support coefficient
dIp	active current recovery slope

References

1. Fu, B.B.; Jia, C.R.; Yang, C.H. Parameter identification of distributed photovoltaic power generation system. *Proc. CSU-EPSA* **2013**, *25*, 116–120.
2. Wang, L.; Shen, S.D.; Zhu, S.Z. A method of time domain identification based of EE model for the excitation system parameters. *Autom. Electr. Power Syst.* **2002**, *8*. [CrossRef]
3. Jiang, P.; Dai, L.F.; Huang, T. Application of frequency domain method in parameter identification for excitation systems of generators. *Autom. Electr. Power Syst.* **2001**, *16*, 30–33.
4. Li, Z.; Zhen, S.; Zhen, X.Q. System identification of adaptive reduced order based on PSO algorithm. *Ind. Control Comput.* **2017**, *30*, 112–115.
5. Wu, S.J.; Chen, J.; Yang, Y. Improved frequency domain synchronous generator parameters identification method based on ant colony optimization. *Shaanxi Electr. Power* **2008**, *44*, 38–42.

6. Yang, S.B.; Wu, M.L. Power load and parameter identification based on improved ant colony algorithm for passenger lines. *Proc. CSEE* **2015**, *35*, 1578–1585.
7. Zhong, W.P. Parameter identification of salient pole permanent magnet synchronous motor based on genetic algorithm. *Proc. CSU-EPSA* **2019**. In press.
8. Xiong, X.F.; Chen, K.; Zhen, W. Photovoltaic inverter model identification based on least squares method. *Power Syst. Prot. Control* **2012**, *40*, 52–57.
9. Liu, L.F. Parameter identification of generators for large power system dynamic equivalence. Master's Thesis, Wuhan University, Wuhan, China, 2004.
10. Dong, W.Q.; Li, Y.J.; Xiang, J. Optimal sizing of a stand-alone hybrid power system based on battery/hydrogen with an improved ant colony optimization. *Energies* **2016**, *9*, 785. [CrossRef]
11. Malik, S.; Kim, D. Prediction-learning algorithm for efficient energy consumption in smart buildings based on particle regeneration and velocity boost in particle swarm optimization neural networks. *Energies* **2018**, *11*, 1289. [CrossRef]
12. Zhu, M.X.; Li, J.C.; Chang, D.G. Optimization of antenna array deployment for partial discharge localization in substations by hybrid particle swarm optimization and genetic algorithm method. *Energies.* **2018**, *11*, 1813. [CrossRef]
13. Zang, X.M.; Chen, Q.; Shan, X. Frequency parameter identification and impact analysis of load based on measured data. *Proc. CSU-EPSA* **2019**. In press.
14. Mao, X.M.; Cai, Y.Z.; Zhao, Y. Excitation system parameter identification via maximum-minimum ant system. *Proc. CSU-EPSA* **2015**, *27*, 51–55.
15. Sun, W.; Kong, X.Y.; Zhang, K. Simulation parameter identification method for generator speed governor system with measured data. *Proc. CSU-EPSA* **2014**, *26*, 26–30.
16. Zhang, X.H.; Lin, H.J.; Liu, M.Z. Model parameters identification of UKF algorithm based on ACO-PSO. *Autom. Electr. Power Syst.* **2014**, *38*, 44–50.
17. Sun, Y.X. Research on the model and parameter identification method of photovoltaic array. Master's Thesis, South China University of Technology, Guangzhou, China, 2018.
18. Xu, Y.; Gao, Z.; Zhu, X.R. Multi-scenario parameters identification of photovoltaic array based on hybrid artificial fish swarm and frog leaping algorithm. *Renew Energy* **2018**, *36*, 519–526.
19. Gao, Z. Study on Parameter identification algorithms of PV array and equivalent model of PV power station. Master's Thesis, North China Electric Power University, Beijing, China, 2018.
20. Zhang, J.J.; Sun, Y.J.; Liu, M.Y. Research on modeling of micro-grid based on data testing and parameter identification. *Energies* **2018**, *11*, 2525. [CrossRef]
21. Kong, X.P.; Yuan, Y.B.; Ruan, S.H. Controller parameter identification of the grid connected PV inverter for fault transient modeling. *Power Syst. Prot. Control* **2017**, *45*, 65–72.
22. Huang, Q.X.; Sun, L.X.; Zhen, W. Ant colony optimization algorithm and disturbance analysis of synchronous generator parameter identification. *Electr. Power Autom. Equip.* **2009**, *29*, 50–53.
23. Wu, M. Research on the particle swarm optimization algorithm. *Manag. Technol. SME* **2018**, *12*, 167–168.